Interaction of pharmacologically active pyrone and pyridinone vanadium(IV,V) complexes with cytochrome *c*

Valeria Ugone[a], Federico Pisanu[b], Eugenio Garribba[b,*]

[a] Istituto di Chimica Biomolecolare, Consiglio Nazionale delle Ricerche, Trav. La Crucca 3, I-07100 Sassari, Italy

[b] Dipartimento di Medicina, Chirurgia e Farmacia, Università di Sassari, Viale San Pietro, I-07100 Sassari, Italy

* Corresponding author.
E-mail address: garribba@uniss.it

Abstract

The interaction between cytochrome *c* (Cyt) and potential vanadium drugs, formed by 1,2-dimethyl-3-hydroxy-4(1*H*)-pyridinonate (dhp) and maltolate (ma), was studied by ElectroSpray Ionization-Mass Spectrometry (ESI-MS). Since under physiological conditions redox processes are possible, the binding of the complexes in the oxidation state +IV and +V, $[V^{IV}O(dhp)_2]$, $[V^{IV}O(ma)_2]$, $[V^{V}O_2(dhp)_2]^-$ and $[V^{V}O_2(ma)_2]^-$, was examined. In all systems $V^{IV,V}$–L–Cyt adducts are observed, their formation depending on V oxidation state, ligand and metal concentration. The larger stability of vanadium(IV) than vanadium(V) complexes favors the interaction of the moieties $V^{IV}OL_2$ and $V^{IV}OL^+$ with V^{IV}, while with V^{V} adducts with $V^{V}O_2L$ and $V^{V}O_2^+$ ion are observed. The analysis of the protein structure suggests that Glu4, Glu21, Asp50, Glu62, Glu66 and Glu104 are the most plausible candidates for monodentate coordination, while the couples (Asp2, Glu4), (Glu92, Glu93) and (His33, Glu104) for bidentate binding. The values of $E_{1/2}$ for $[V^{IV}O(dhp)_2]$ and $[V^{IV}O(ma)_2]$, measured by cyclic voltammetry (CV), 0.53 V and 0.60 V vs. standard hydrogen electrode, indicate that an oxidation of V^{IV} to V^{V} is possible. The presence of a protein can alter the redox reactions and stabilize one of the states, V^{IV} or V^{V}. Overall, the data reinforce the conclusion that, for V drugs, the biotransformation is fundamental to explain their biological action and the analysis should not be limited to the ligand exchange and hydrolysis but also include the redox processes, and that a mixture of V^{IV} and V^{V} species, $V^{IV,V}$–L–Protein and $V^{IV,V}$–Protein, could be responsible of the pharmacological effects.

Keywords

Vanadium, potential drugs, protein binding, redox reactions, ESI-MS spectrometry

1. Introduction

Over the last years, vanadium compounds have been extensively studied for their pharmacological properties and potential use in medicine as antiparasitic [1], antibacterial [2], but – mainly – as antidiabetic [3-7] and anticancer [8-16] drugs.

After *in vitro* or *in vivo* studies, several vanadium(IV) and vanadium(V) compounds have shown interesting properties [6, 9, 13, 15, 17]. Species with stoichiometry $V^{IV}OL_2$ [18] and $V^{V}O_2L_2$ [19, 20], where L is a bidentate and monoanionic ligand, have been extensively tested. Among the compounds with stoichiometry $V^{IV}OL_2$, bis(maltolato)oxidovanadium(IV) (BMOV) and bis(ethylmaltolato)oxidovanadium(IV) (BEOV) are worth of being mentioned and are considered the benchmark complexes for new molecules with anti-diabetic action [3]. Maltol (3-hydroxy-2-methyl-4*H*-pyran-4-one; ma) is a naturally occurring compound used as a food additive to enhance the flavor of breads and cakes. The story of BMOV as potential anti-diabetic agent starts at the beginning of the 90s of the last century, when it was demonstrated that it normalizes glucose and lipid values without increasing insulin levels. Its derivative BEOV, under the name AKP020, completed phases I and IIa of clinical trials [3, 4], but the tests were blocked for two reasons, the renal problems of several patients and financial problems of Akesis Pharmaceuticals [21, 22]. After the synthesis of BMOV, the anti-diabetic potential of other $V^{IV}O$ compounds with O_4 and N_2O_2 coordination was examined. One promising $V^{IV}O$ complex is formed by 1,2-dimethyl-3-hydroxy-4(1*H*)-pyridinone (deferiprone or dhp), with formula $[V^{IV}O(dhp)_2]$; it is a strong inhibitor of fatty acid mobilization and is effective in the treatment of rats affected by diabetes induced with streptozotocin (STZ) [23]. $[V^{IV}O(dhp)_2]$ can be considered a bridge between the two major applications proposed for vanadium species, since it shows, besides the anti-diabetic action, anti-cancer effectiveness as well; in fact, it is active against malignant melanoma cells and causes apoptosis and cell cycle block [24].

In the development and design of the metallodrugs, and in particular of those based on vanadium, the major challenge concerns the understanding of the mechanisms of action, not yet fully known, and the identification of active species in order to obtain more effective compounds and reduce their toxicity and possible side effects. Indeed, under physiological conditions, the vanadium complexes give extensive hydrolysis, ligand exchange and redox reactions, as well as changes in geometry and coordination number. It has been pointed out that the scarce interest of the pharmaceutical companies for the development of vanadium-based drugs can be related to the limited knowledge of their biospeciation in the organism [25].

One of the less studied and understood aspects of the behavior of V potential drugs are the redox processes. Up to now it is unclear if, in the biological fluids, is favored the oxidation or, in contrast,

the reduction. On one hand the oxidation of $V^{IV}O^{2+}$ ion to V^{V} occurs very easily around physiological pH in aqueous solution [26]. Harris and co-workers suggested that the O_2 concentration in the blood not bound to hemoglobin (that varies from 100 mm Hg in the lungs and arteries to 40 mm Hg in the blood vessels and peripheral tissues) could be sufficient to oxidize V^{IV} to V^{V} and determined a time of 1-4 h for the oxidation *in vivo* of $V^{IV}O$–transferrin adducts [27]. Another oxidant may be hydrogen peroxide, which could oxidize $V^{IV}O$ compounds with the formation of hydroxyl radicals ($^{\bullet}OH$) *via* a Fenton-like reaction, even if contrasting opinions on its amount in biological fluids have been reported [28-30]. On the other hand, the reduction may be promoted by reducing agents like reduced glutathione (GSH), cysteine (Cys), L-ascorbate (Asc) and reduced nicotinamide adenine dinucleotide and nicotinamide adenine dinucleotide phosphate (NADH and NADPH) [31-34]. In human erythrocytes and rat adipocytes, GSH – present in the cytosol in high concentration (2.3 mM) – reduces V^{V} to $V^{IV}O^{2+}$ which is subsequently complexed by several bioligands [35, 36]. Through blood circulation monitoring-electron paramagnetic resonances (BCM-EPR) experiments, it has been demonstrated that the larger amount of vanadium in the blood, when it is administered as $V^{IV}OSO_4$, exists in the oxidation state +IV [37]. Therefore, even though there is no unanimous consensus on the V oxidation state at the physiological conditions, an interconversion between the states +IV and +V is likely in serum and cytosol and, depending on the specific V species, an equilibrium between the concentration of V^{IV} and V^{V} may be reached [11, 27, 38-43]. This would account for the similar effects exerted by V^{IV} and V^{V} compounds.

In this scenario, the interaction with proteins of vanadium potential drugs, in both the oxidation states, could play a very important role in their transport in organism and mechanism of action [44]. The binding depends on various factors: the structure of the V species in aqueous solution, its thermodynamic stability, the presence of accessible residues on the protein surface, the stabilization of the adduct by hydrogen bonds (H-bonds) or van der Waals (vdW) contacts [44, 45]. Moreover, the interaction can be covalent with the direct binding of one or more amino acid side-chains to the first coordination sphere of vanadium or non-covalent with only secondary contacts on the second coordination sphere [44, 46]. In addition, such types of binding to proteins could stabilize one of the two oxidation states +IV or +V and, therefore, determine the active species in the organism.

Over the last years, a growing number of papers dealt with the interaction of vanadium compounds both with large proteins like human serum transferrin in the apo or holo form [47-52], human serum albumin [52-55], hemoglobin [47, 56], immunoglobulin G [47, 57], and small proteins, such as lysozyme [58-61], myoglobin [62] and ubiquitin [59, 60, 63] and ribonuclease A [64]. These systems were investigated through the integrated application of several techniques such as X-ray

diffraction, ESI-MS, NMR, EPR, UV–vis and CD spectroscopy as well as computational methods. Small proteins play a special role in this kind of works: on one hand they are important for the intrinsic physiological functions, on the other they can be considered models easily analyzable for the limited dimensions and number of potential sites and to get information on larger and more complex proteins [65].

In this study, the binding of V^{IV} and V^{V} complexes formed by 1,2-dimethyl-3-hydroxy-4(1*H*)-pyridinone (dhp) and maltol (ma), $[V^{IV}O(dhp)_2]$, $[V^{V}O_2(dhp)_2]^-$, $[V^{IV}O(ma)_2]$, $[V^{V}O_2(ma)_2]^-$, with cytochrome *c* (Cyt) was evaluated by ElectroSpray Ionization-Mass Spectrometry (ESI-MS) technique. In aqueous solution, at mM concentration, $[V^{IV}O(dhp)_2]$ exists as a mixture of $[V^{IV}O(dhp)_2]$ and $[V^{IV}O(dhp)_2(H_2O)]$ in equilibrium, while $[V^{IV}O(ma)_2]$ forms the *cis*-octahedral species $[V^{IV}O(ma)_2(H_2O)]$ (Scheme 1). Cytochrome *c* is a small protein (104 amino acids, MM < 12400 Da) suitable for ESI-MS studies since it produces well-resolved spectra in the m/z 1000-2000 range [66]. It has important biological functions being involved in the electron transport chain in mitochondria and playing a crucial role in the cellular apoptosis pathway [67]. As pointed out in the literature, the apoptotic function of Cyt could be exploited in the development of new drugs, including metal drugs; the types of cancer receptive to the protein cytotoxicity and the factors which can be tuned to increase its pharmacological efficiency have been identified [68]. Recently, the interaction between Cyt and anti-bacterial $[V^{IV}O(nalidixato)_2(H_2O)]$ has been described and both covalent and non-covalent binding of $V^{IV}O(nalidixato)_2$ moiety has been demonstrated, with the residues Glu21 and Glu90 being involved in the metal binding [46]. Therefore, this study could throw light on the interaction of other pharmacologically active V^{IV} and V^{V} complexes with Cyt and on the eventual differences of the metal oxidation states in the protein binding.

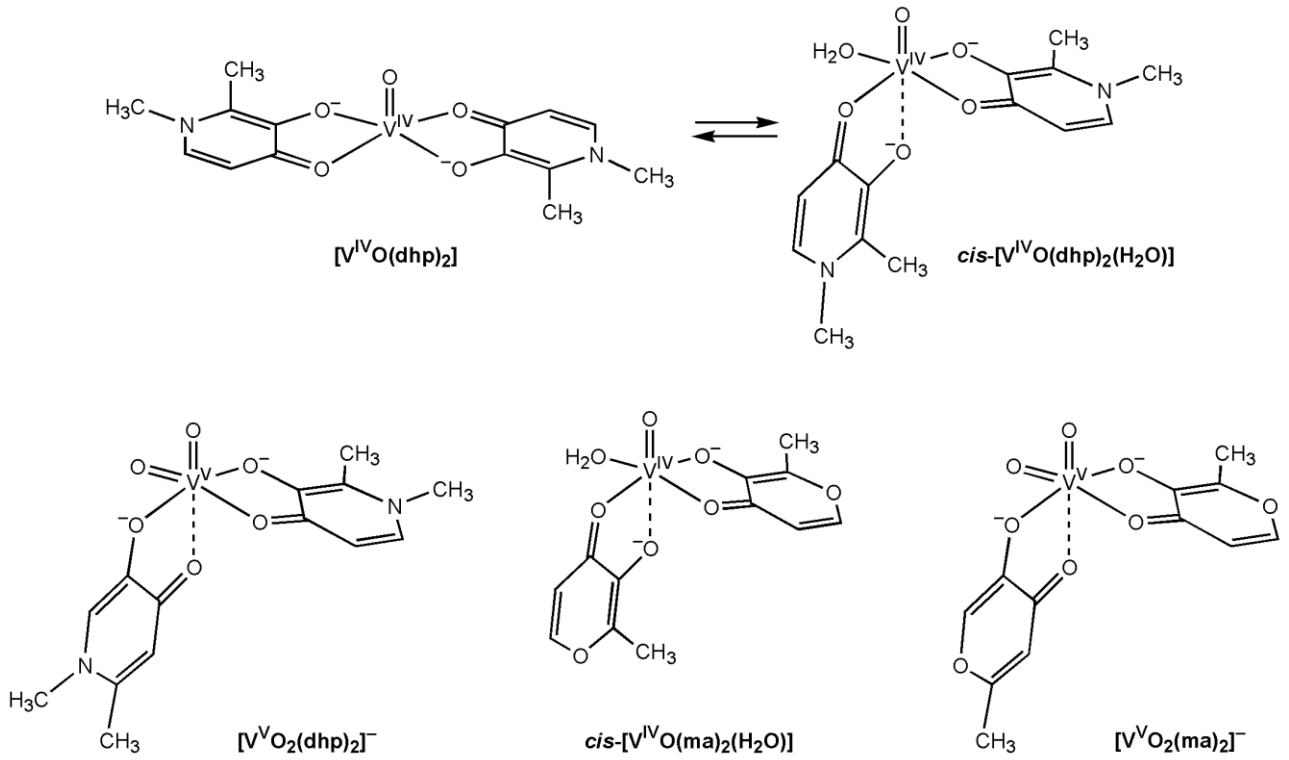

Scheme 1. Structure in aqueous solution of the $V^{IV,V}$ complexes formed by dhp and ma examined in this study.

2. Material and methods

2.1. Chemicals

Water was deionized through the purification system Millipore MilliQ Academic or purchased from Sigma-Aldrich (LC-MS grade). The chemicals oxidovanadium(IV) sulfate trihydrate ($V^{IV}OSO_4 \cdot 3H_2O$), ammonium vanadate ($NH_4V^VO_3$), 1,2-dimethyl-3-hydroxy-4(1*H*)-pyridinone (deferiprone, dhp), 3-hydroxy-2-methyl-4*H*-pyran-4-one (maltol, ma), cytochrome *c* from equine heart (Cyt, C2506) were Sigma-Aldrich products of the highest grade available and were used as received.

The complexes $[V^{IV}O(dhp)_2]$ and $[V^{IV}O(ma)_2]$ were synthesized following the procedure established in the literature [69, 70].

2.2. ESI-MS Measurements

The solutions for ESI-MS measurements were prepared as follows. Briefly, the solid V^{IV} complexes or $NH_4V^VO_3$ plus the ligands in molar ratio 1/2 were dissolved in LC-MS grade water to obtain a V concentration of 1.0-2.0 mM. Argon was bubbled in the systems containing V^{IV} in order to avoid the oxidation. Subsequently, the solutions were diluted up to a V concentration of 50 μM and the

ESI-MS spectra were immediately acquired.

The samples of the ternary systems containing cytochrome *c* were prepared mixing a proper amount of the V solution with an aliquot of a stock protein solution (500 μM) to reach (V complex)/Cyt ratios of 3/1 or 5/1 and a protein concentration of 5 or 50 μM. In all the solutions pH was in the range 5-6. ESI-MS spectra were acquired immediately after the preparation of the solutions.

Mass spectra in the positive- or negative-ion mode were recorded on a Q Exactive Plus Hybrid Quadrupole-Orbitrap (Thermo Fisher Scientific) mass spectrometer. The solutions were infused at a flow rate of 5.00 μL/min into the ESI chamber. The spectra were obtained in the m/z range 50-750 for the binary systems and 300–4500 in the systems containing the protein, with a resolution of 140000, and accumulated for at least 5 min to increase the signal-to-noise ratio. The instrumental setting for the spectra measurements in positive-ion mode was as follows: spray voltage 2300 V, capillary temperature 250 °C, sheath gas 10 (arbitrary units), auxiliary gas 3 (arbitrary units), sweep gas 0 (arbitrary units), probe heater temperature 50 °C. The setting used for negative-ion mode spectra was as follows: spray voltage −1900 V, capillary temperature 250 °C, sheath gas 20 (arbitrary units), auxiliary gas 5 (arbitrary units), sweep gas 0 (arbitrary units), probe heater temperature 14 °C. ESI-MS spectra were analyzed by using Thermo Xcalibur 3.0.63 software (Thermo Fisher Scientific) and the average deconvoluted monoisotopic masses were obtained through the Xtract tool integrated in the software.

2.3. Electrochemistry

Cyclic voltammetry (CV) measurements (CVon the systems with $[V^{IV}O(dhp)_2]$ and $[V^{IV}O(ma)_2]$ were obtained with an electrochemical analyzer CH Instruments 600 B at room temperature (25 ± 1 °C) in H_2O with 0.1 M KCl, as reported previously [71]. The total $V^{IV}O$ concentration was 1 mM. A glassy carbon working electrode, a Pt wire counter electrode and a reference saturated calomel electrode (SCE, Hg/Hg_2Cl_2) were employed. All potentials were calculated relative to the Hg/Hg_2Cl_2 electrode (0.224 V vs. standard hydrogen electrode (SHE) at 25 °C), with a value of +0.22 V for the $[Fe^{III}(CN)_6]^{3-}/[Fe^{II}(CN)_6]^{4-}$ couple (0.01 M NaOH). Voltammograms were obtained at scan rates between 0.1 and 1 V s^{-1}. Redox potentials were determined with a precision of ±0.01 V.

2.4. Analysis of the protein structure

The structure of cytochrome *c* was downloaded from Protein Data Bank (PDB) [72, 73] with code 1HRC [74]. The analysis of its structure, in particular the possible binding sites consisting of Asp, Glu and His residues, was carried out with the software Swiss-Pdb Viewer, version 4.1.0 [75].

3. Results and discussion

3.1. Binary systems $V^{IV}O$/dhp and $V^{V}O_2$/dhp

1,2-Dimethyl-3-hydroxy-4(1*H*)-pyridinone is used to treat iron overload in *Thalassaemia major* by chelation therapy, due to the formation of stable complexes with Fe^{III} [76]. Similarly, it can form stable chelate complexes with vanadium in different oxidation states.

The complex $[V^{IV}O(dhp)_2]$ is penta-coordinated with a square pyramidal geometry in the solid state [77]. In aqueous solution $[V^{IV}O(dhp)_2]$ is in equilibrium with *cis*-$[V^{IV}O(dhp)_2(H_2O)]$, with a H_2O molecule adjacent to the oxido ligand (Scheme 1), and the position of the equilibrium is influenced by the experimental conditions such as the temperature [69, 78, 79]. *cis*-$[V^{IV}O(dhp)_2(H_2O)]$ undergoes deprotonation of the equatorial water molecule to give the corresponding mono-hydroxido species *cis*-$[V^{IV}O(dhp)_2(OH)]^-$ with a p*K* of 10.59 [69]. The existence of the bis-chelated species around the physiological pH was confirmed by ESI-MS that shows the signals of $[V^{IV}O(dhp)_2+H]^+$ at m/z 344.06 and $[V^{IV}O(dhp)_2+Na]^+$ at m/z 366.04 [80].

The ligand dhp forms stable complexes with V^V as well. The structure at the solid state, $K[V^{V}O_2(dhp)_2]\cdot 2H_2O$, has been solved by single crystal X-ray diffraction analysis; it shows two monoanionic ligands bound to *cis*-$V^{V}O_2^+$ ion with (O_{keto}, O_{phen}^-) coordination [81] (see Scheme 1). In the same study, the stability constants have been determined by pH-metric and ^{51}V NMR measurements [81]. With increasing pH, $[V^{V}O_2(dhp)]$, $[V^{V}O_2(dhp)_2]^-$, $[V^{V}O(dhp)_2(OH)]$ and $[V^{V}O_2(dhp)(OH)]^-$ have been determined before the formation of $[HV^{V}O_4]^{2-}$ which occur after pH 10; among them, $[V^{V}O_2(dhp)(OH)]^-$ and $[V^{V}O_2(dhp)_2]^-$ are the major species in solution at the physiological pH.

The negative-mode ESI-MS spectrum recorded on the system $V^{V}O_2^+$/dhp with a 1/2 molar ratio is depicted in Figure 1, where the peaks at m/z 237.99 and 359.05 were attributed to $[V^{V}O_2(dhp)(OH)]^-$ and $[V^{V}O_2(dhp)_2]^-$, respectively, in good agreement with the pH-potentiometric measurements. The comparison between the experimental and calculated isotopic pattern for the peak of $[V^{V}O_2(dhp)_2]^-$ ion is shown in Figure 2 as an example. The same species were detected in positive mode as H^+ or Na^+ adducts (see Table 1). Moreover, the presence of di- and trinuclear complexes, $[(V^{V}O_2)_2(dhp)O]^-$ (m/z 319.92), $[(V^{V}O_2)_2(dhp)_2(OH)]^-$ (m/z 458.98) and $[(V^{V}O_2)_3(dhp)_3(OH)]^-$ (m/z 679.97) was observed. Among the most intense peaks revealed in the ESI-MS(–) spectrum, those of the free mono- and tetranuclear vanadate(V) were identified at m/z 116.94 and 198.87 (Figure 1), indicating that the V^V–dhp complexes are partly hydrolysed at these experimental conditions.

In the ESI-MS(+) spectrum, the more intense peaks are those of the adducts of the free ligand with

protons and sodium ions. The peaks of the metal species are much less intense than in the negative-mode spectra due to the negative charges of the major species in solution (Table 1). However, monooxido V^V species were detected, such as $[V^VO(dhp)_2]^+$ (m/z 343.05) and $[V^VO(dhp)_2(OH)+Na]^+$ (m/z 383.04), which confirm the formation of $[V^VO(dhp)_2(OH)]$, identified by pH-potentiometry at acidic pH in the system V^V/dhp 1/3 [81].

All the species revealed in the mass spectra are listed in Table 1.

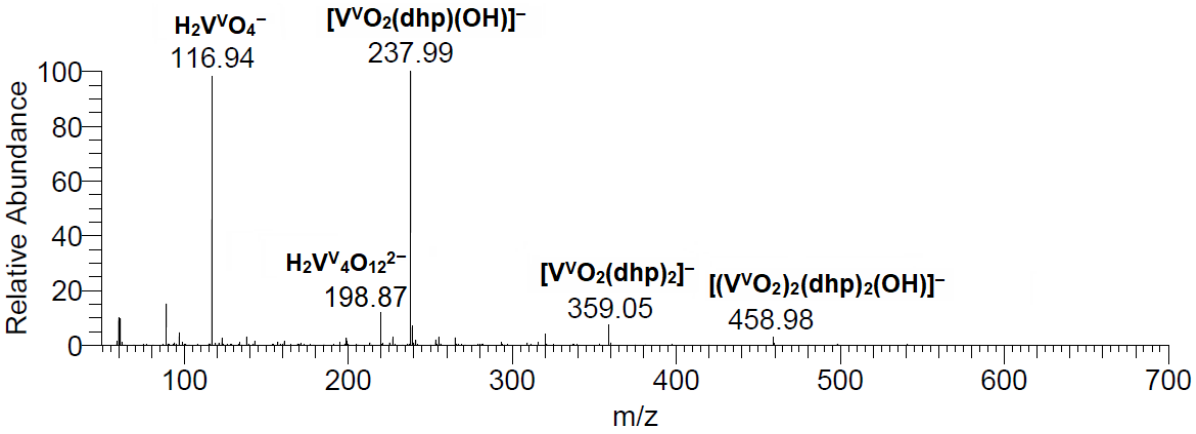

Figure 1. ESI-MS(–) spectrum of the system $V^VO_2^+$/dhp 1/2 (V concentration 50 µM) in ultrapure LC/MS water.

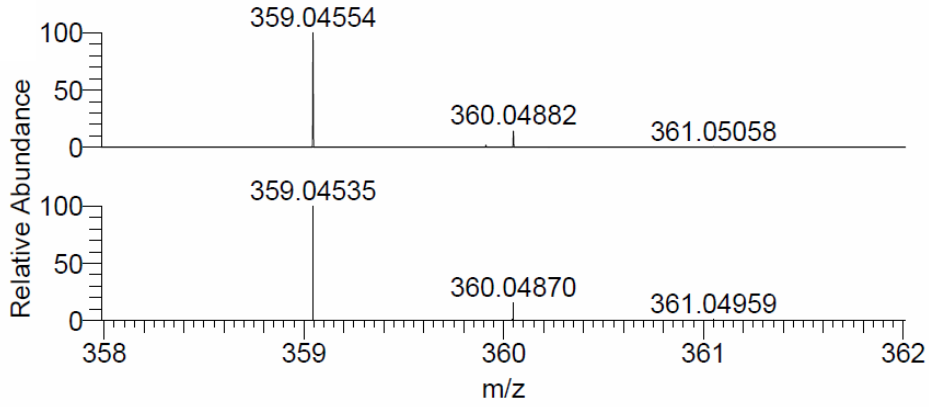

Figure 2. Experimental (top) and calculated (bottom) isotopic pattern of the species $[V^VO_2(dhp)_2]^-$.

Table 1. Identified species in the ESI-MS spectra of the system $V^VO_2^+$/dhp.

Ion	Composition	Experimental (m/z)[a]	Calculated (m/z)[a]	Error (ppm) [b]
dhp^-	$C_7H_8NO_2$	138.05492	138.05605	–8.2
$[V^VO_2(dhp)(OH)]^-$	$C_7H_9NO_5V$	237.99230	237.99258	–1.2

$[V^{V}O_2(dhp)_2]^-$	$C_{14}H_{16}N_2O_6V$	359.04554	359.04535	0.5
$[V^{V}O_2(dhp)–H]^-$	$C_7H_7NO_4V$	219.98156	219.98202	–2.1
$[(V^{V}O_2)_2(dhp)O]^-$	$C_7H_8NO_7V_2$	319.91855	319.91855	0.0
$[(V^{V}O_2)_2(dhp)_2(OH)]^-$	$C_{14}H_{17}N_2O_9V_2$	458.98217	458.98188	0.6
$[(V^{V}O_2)_3(dhp)_3(OH)]^-$	$C_{21}H_{25}N_3O_{13}V_3$	679.97203	679.97118	1.3
$H_2VO_4^-$	H_2O_4V	116.93857	116.93982	–10.7
$H_2V_4O_{12}^{2-}$	$H_2O_{12}V_4$	198.86513	198.86579	–3.3
$[Hdhp+H]^+$	$C_7H_{10}NO_2$	140.07046	140.07061	–1.1
$[Hdhp+Na]^+$	$C_7H_9NO_2Na$	162.05236	162.05255	–1.2
$[V^{V}O_2(dhp)+H]^+$	$C_7H_9NO_4V$	221.99631	221.99657	–1.2
$[V^{V}O_2(dhp)+Na]^+$	$C_7H_8NO_4VNa$	243.97827	243.97852	–1.0
$[V^{V}O(dhp)_2]^+$	$C_{14}H_{16}N_2O_5V$	343.04903	343.04934	–0.9
$[V^{V}O(OH)(dhp)_2+Na]^+$	$C_{14}H_{17}N_2O_6VNa$	383.04154	383.04185	–0.8

[a] Experimental and calculated m/z values refer to the peak representative of the monoisotopic mass.

[b] Error in ppm compared to the experimental value, calculated as: 10^6 × [Experimental (m/z) – Calculated (m/z)] / Calculated (m/z).

3.2. Ternary systems $V^{IV}O$/dhp/Cyt and $V^{V}O_2$/dhp/Cyt

The interaction with Cyt of $[V^{IV}O(dhp)_2]$/$[V^{IV}O(dhp)_2(H_2O)]$ and $[V^{V}O_2(dhp)_2]^-$ has been investigated by recording ESI-MS spectra in ultrapure water varying the molar ratio between the complex and protein (3/1 and 5/1) and Cyt concentration (5 or 50 μM).

First, the raw spectrum of the free protein, recorded as a reference (Figure S1), shows a characteristic pattern dominated by the species with +8 charge (m/z = 1545.8), between those with + 9 (m/z = 1378.4) and +7 (m/z = 1766.5); the relative intensities are in agreement with the literature data [66, 82]. In the deconvoluted spectrum, it is possible to observe the main signal corresponding to the mass of Cyt (12358.3 Da) and the series of signals due to the adducts between the protein and ubiquitous ions like Na^+ and K^+ (Figure S1).

The mass spectra of the ternary systems are characterized by a distribution of the charged species that does not vary significantly after the V binding, indicating that the protein conformation remains (almost) the same [83, 84]. As an example, some raw spectra recorded on the solutions containing $V^{IV}O^{2+}$/dhp and Cyt are reported in Figure S2.

The deconvoluted spectra of Cyt 5 μM in presence of $[V^{IV}O(dhp)_2]$/$[V^{IV}O(dhp)_2(H_2O)]$ show peaks at +205 Da and +343 Da, compared to the free protein (12358 Da), which are consistent with the

mass of the moieties $V^{IV}O(dhp)$ and $V^{IV}O(dhp)_2$, respectively (Figure S3). All the detected adducts and their masses are listed in Table 2. At higher concentration, Cyt 50 µM, the spectra suggest that several different $V^{IV}O$ fragments are bound to the protein (Figure 3): i) $n[V^{IV}O(dhp)]$ with n = 1-2; ii) $n[V^{IV}O(dhp)(H_2O)]$ with n = 1-2; iii) $n[V^{IV}O(dhp)_2]$ with n = 1-3; iv) $\{n[V^{IV}O(dhp)_2]+[V^{IV}O(dhp)]\}$ with n = 1-3; v) $\{n[V^{IV}O(dhp)_2]+[V^{IV}O(dhp)(H_2O)]\}$ with n = 1, 2. Notably, in all the spectra, the additional peak of the adduct $[V^{V}O_2]$–Cyt (12440 Da) is revealed. This indicates that a partial oxidation of V^{IV} to V^{V} occurs in solution or during the ionization process.

Table 2. Adducts detected in the systems $V^{IV}O$/dhp/Cyt and $V^{V}O_2$/dhp/Cyt.

Adduct	Experimental mass (Da)	Expected mass (Da)[a]
$[V^{IV}O(dhp)]$–Cyt	12562.3	12563.3
$[V^{IV}O(dhp)(H_2O)]$–Cyt	12579.3	12581.3
$[V^{IV}O(dhp)_2]$–Cyt	12701.4	12701.3
$2[V^{IV}O(dhp)]$–Cyt	12767.3	12768.3
$\{[V^{IV}O(dhp)]+[V^{IV}O(dhp)(H_2O)]\}$–Cyt	12784.3	12786.3
$\{[V^{IV}O(dhp)_2]+[V^{IV}O(dhp)]\}$–Cyt	12905.4	12906.3
$\{[V^{IV}O(dhp)_2]+[V^{IV}O(dhp)(H_2O)]\}$–Cyt	12922.4	12924.4
$2[V^{IV}O(dhp)_2]$–Cyt	13045.4	13044.4
$\{2[V^{IV}O(dhp)_2]+[V^{IV}O(dhp)]\}$–Cyt	13249.4	13249.4
$\{2[V^{IV}O(dhp)_2]+[V^{IV}O(dhp)(H_2O)]\}$–Cyt	13266.4	13267.4
$3[V^{IV}O(dhp)_2]$–Cyt	13388.5	13387.4
$[V^{V}O_2]$–Cyt	12440.3	12441.2
$[V^{V}O_2(dhp)]$–Cyt	12579.3	12579.3
$2[V^{V}O_2(dhp)]$–Cyt	12800.3	12800.3
$3[V^{V}O_2(dhp)]$–Cyt	13022.3	13021.3

[a] The expected mass is obtained by summing the exact mass of the vanadium moiety to the experimental mass of the free protein (12358.3 Da).

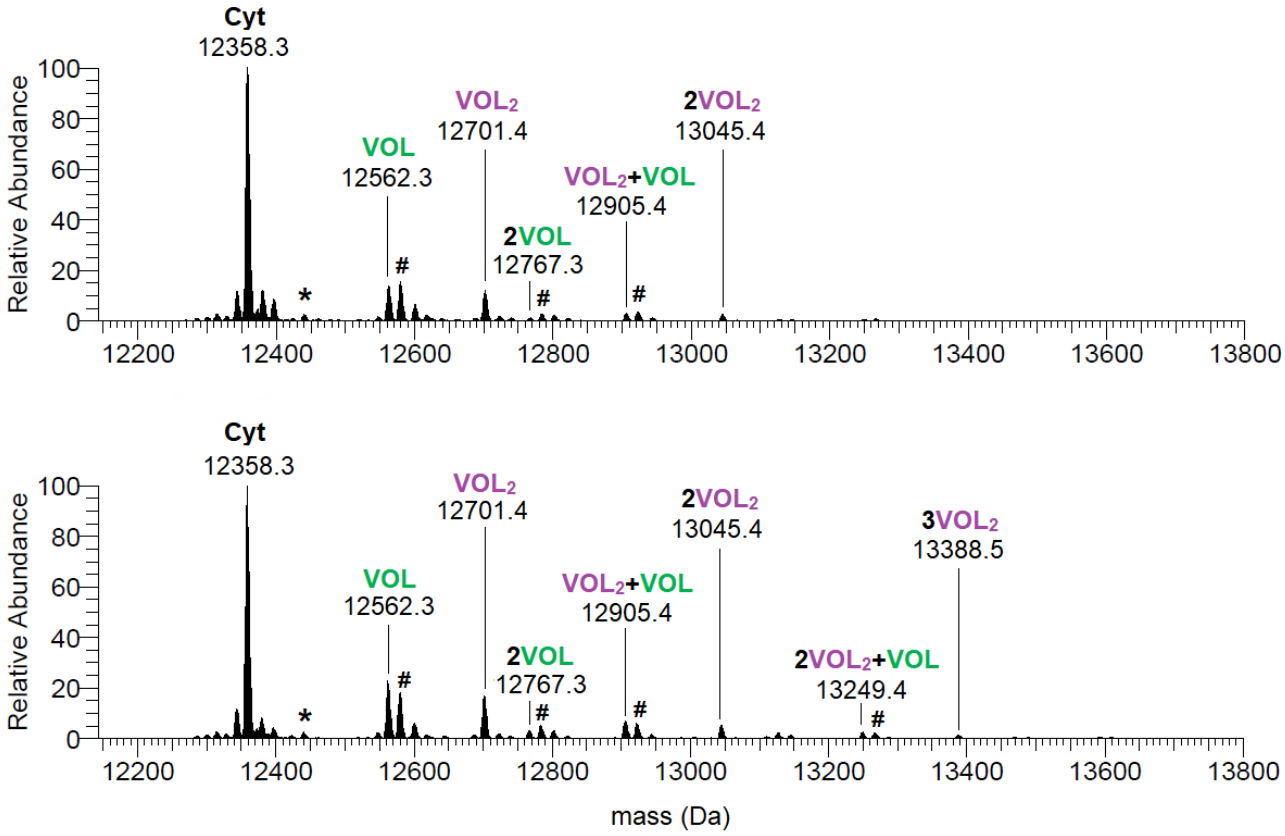

Figure 3. Deconvoluted ESI-MS spectra recorded on the system containing $V^{IV}O^{2+}$/dhp 1/2 and cytochrome *c* (50 μM): V/Protein molar ratio 3/1 (top) and 5/1 (bottom). L indicates the dhp ligand. With the asterisk the peak of the adduct $[V^{V}O_2]$−Cyt is denoted. With the hash symbols the signals of the adducts with an additional H_2O molecule with respect to the adjacent peak are indicated.

In the spectra recorded in the systems containing $V^{V}O_2$/dhp/Cyt, a group of peaks at higher mass values than Cyt alone suggests the formation of protein−(metal species) adducts. In particular, when the protein concentration is 5 μM, the signals of $[V^{V}O_2(dhp)]$−Cyt and $2[V^{V}O_2(dhp)]$−Cyt adducts were detected at 12579 Da and 12800 Da (Figure 4), while with a protein concentration of 50 μM, up to 3 $V^{V}O_2$(dhp) fragments bind to the protein (Figure 5). The mass of the $V^{V}O_2$(dhp) moiety is 221 Da. As observed with the corresponding system with V^{IV}, a small peak at 12440-12441 m/z, attributable to the adduct $[V^{V}O_2]$–Cyt, was revealed (Figure 4). It can be noticed that increasing the V/Protein molar ratio the number of signals is almost the same, with a little increment of the intensities of the (V species)–Cyt peaks.

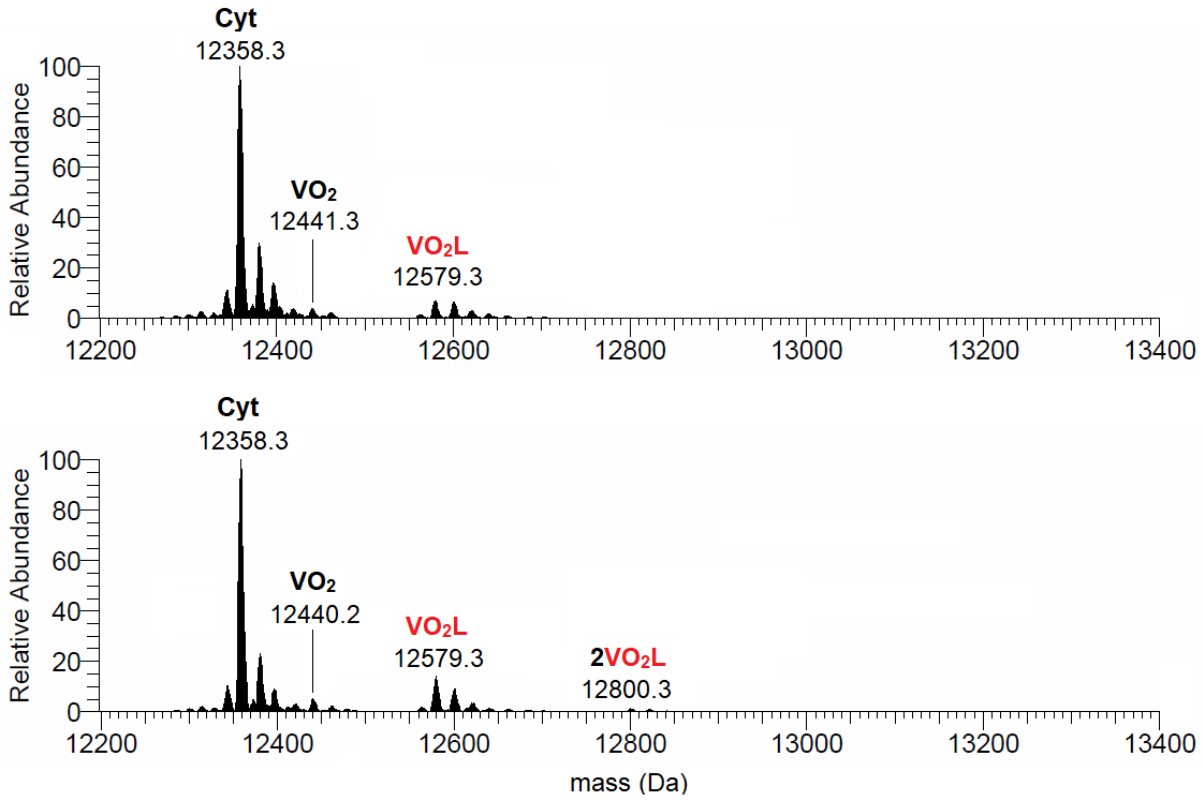

Figure 4. Deconvoluted ESI-MS spectra recorded on the system containing $V^{V}O_2^+$/dhp 1/2 and cytochrome *c* (5 µM): V/Protein molar ratio 3/1 (top) and 5/1 (bottom). L indicates the dhp ligand.

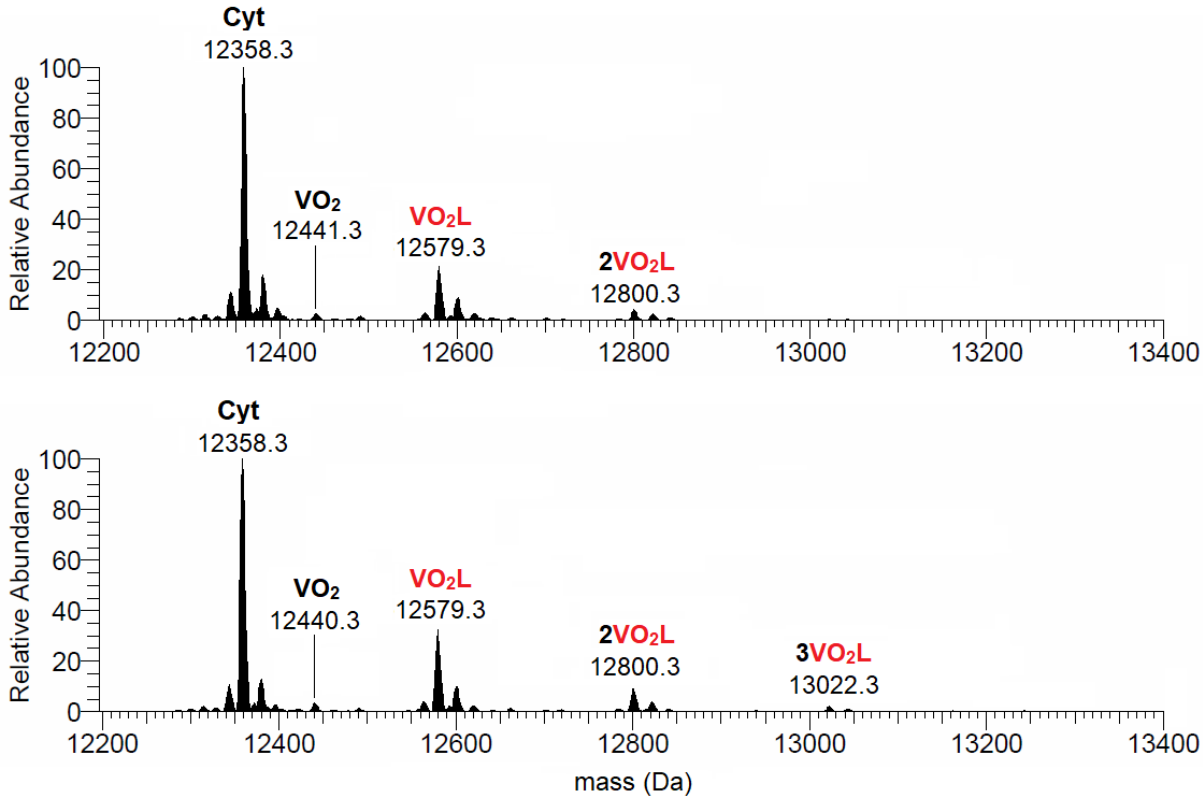

Figure 5. Deconvoluted ESI-MS spectra recorded on the system containing $V^{V}O_2^+$/dhp 1/2 and cytochrome *c* (50 µM): V/Protein molar ratio 3/1 (top) and 5/1 (bottom). L indicates the dhp ligand.

3.3. Binary systems $V^{IV}O$/ma and $V^{V}O_2$/ma

Maltol forms stable complexes with V^{IV} and V^{V}. With $V^{IV}O^{2+}$ ion, it forms in solution complexes with stoichiometry $[V^{IV}O(ma)(H_2O)_2]^+$, $[V^{IV}O(ma)_2(H_2O)]$ and $[V^{IV}O(ma)_2(OH)]^-$ [85, 86]. The bis-chelated complex $[V^{IV}O(ma)_2]$ exhibits a square pyramidal geometry in the solid state [70], but in aqueous solution, at millimolar concentration and at physiological pH, it transforms into *cis*-$[V^{IV}O(ma)_2(H_2O)]$ (Scheme 1), the equatorial water undergoing deprotonation with a pK_a of 8.79 [85]. Therefore, this latter and the moieties derived from it can react with the proteins. The formation of this species has been also confirmed recently by ESI-MS(+) studies where the signal of $[V^{IV}O(ma)_2+H]^+$ (m/z = 317.99) was observed [80].

With vanadium(V), the X-ray structure of $K[V^{V}O_2(ma)_2]\cdot H_2O$ has been solved with two ligands coordinated to *cis*-$V^{V}O_2^+$ moiety with the keto-O donors in *trans* position to the oxido groups [70]. Potentiometric and ^{51}V NMR measurements in aqueous solution at different pH revealed that the most important species in pH range 4-8 is $[V^{V}O_2(ma)_2]^-$ [87, 88]. Small amounts of the mono-chelated complexes $[V^{V}O_2(ma)(OH)]^-$ and $[V^{V}O_2(ma)(OH)_2]^{2-}$ were also detected [87, 88].

In this work, the system V^{V}/ma was studied starting from the vanadium(V) salt, $NH_4V^{V}O_3$, in presence of the ligand with a molar ratio 1/2. ESI-MS spectra confirm the presence of the mono-chelated $[V^{V}O_2(ma)(OH)]^-$ (m/z 224.96) and bis-chelated species $[V^{V}O_2(ma)_2]^-$ (m/z 332.98) (Figure S4). The comparison between the experimental and the calculated pattern for the peak of $[V^{V}O_2(ma)_2]^-$ is reported in Figure S5. Table 3 collects all the identified species in the ESI-MS spectra, recorded both in negative- and positive-ion mode. In the negative mode, an intense signal belongs to $H_2V^{V}O_4^-$, as seen in the aforementioned system with dhp, indicating the importance of the hydrolysis at low metal concentration. Compared to the negative-ion mode, the spectra recorded in the positive mode show the presence of less peaks, all assignable to adducts with H^+ or Na^+ ions, and this can be explained with the anionic nature of the V^{V} complexes.

Table 3. Identified species in the ESI-MS spectra of the system $V^{V}O_2^+$/ma.

Ion	Composition	Experimental (m/z)[a]	Calculated (m/z)[a]	Error (ppm) [b]
ma^-	$C_6H_5O_3$	125.02326	125.02442	–9.3
$[V^{V}O_2(ma)_2]^-$	$C_{12}H_{10}O_8V$	332.98247	332.98208	1.2
$[V^{V}O_2(ma)(OH)]^-$	$C_6H_6O_6V$	224.96070	224.96095	–1.1
$[V^{V}O_2(ma)-H]^-$	$C_6H_4O_5V$	206.94990	206.95039	−2.4
$H_2V^{V}O_4^-$	H_2O_4V	116.93861	116.93982	–10.3
$H_2V_4O_{12}^{2-}$	$H_2O_{12}V_4$	198.86519	198.86579	–3.0

$[V^{V}O_2(ma)+H]^+$	$C_6H_6O_5V$	208.96506	208.96494	0.6
$[V^{V}O_2(ma)(H_2O)+H]^+$	$C_6H_8O_6V$	226.97562	226.97550	0.5
$[Hma+H]^+$	$C_6H_7O_3$	127.03918	127.03897	1.7
$[Hma+Na]^+$	$C_6H_6NaO_3$	149.02108	149.02092	1.1

[a] Experimental and calculated m/z values refer to the peak representative of the monoisotopic mass.

[b] Error in ppm respect to the experimental value, calculated as: 10^6 ×[Experimental (m/z) – Calculated (m/z)]/ Calculated (m/z).

3.4. Ternary systems $V^{IV}O$/ma/Cyt and $V^{V}O_2$/ma/Cyt

The mass spectra of the system $V^{IV}O$/ma/Cyt were recorded with Cyt concentration of 5 and 50 μM. As observed in the system with $[V^{IV}O(dhp)_2]$, the comparison of the charge-state distribution in the spectra containing free Cyt and those with the metal complexes suggests that the binding of the vanadium moieties does not cause variations of the conformation of protein [83, 84]. Several adducts were found, collected in Table 4. At low concentration (Cyt 5 μM) and spontaneous pH (values between 5 and 6), the spectra show the presence of the adduct with $V^{V}O_2^+$, derived from the oxidation of the $V^{IV}O^{2+}$ ion, and of a very small amount of $[V^{IV}O(ma)]$−Cyt. With a protein concentration of 50 μM, species with $V^{IV}O^{2+}$ and one or more mono-chelated fragment $V^{IV}O(ma)$ bound to Cyt were identified, in agreement with what was found with other proteins [62, 63, 80]. In particular, the adducts with composition $n[V^{IV}O(ma)]$−Cyt (with n = 1-3 when the ratio V/Cyt is 3/1 and n = 1-5 when the ratio is 5/1) and $\{n[V^{IV}O(ma)]+[V^{IV}O(ma)_2]\}$−Cyt ($n$ = 0–4), less intense than the previous ones, were detected (Figure 6). The additional low intense peaks corresponding to the $V^{IV}O^{2+}$ (12424 Da) and $V^{V}O_2^+$ (12440) adducts suggest the partial hydrolysis and oxidation of the V^{IV} species that could occur in solution or during the ionization process.

Table 4. Adducts detected in the systems $V^{IV}O$/ma/Cyt and $V^{V}O_2$/ma/Cyt.

Adduct	Experimental mass (Da)	Expected mass (Da)[a]
$[V^{IV}O]$–Cyt	12424.3	12425.2
$[V^{IV}O(ma)]$–Cyt	12549.3	12550.3
$[V^{IV}O(ma)_2]$–Cyt	12676.3	12675.3
$2[V^{IV}O(ma)]$–Cyt	12741.3	12742.3
$\{[V^{IV}O(ma)]+[V^{IV}O(ma)_2]\}$–Cyt	12867.3	12867.2
$3[V^{IV}O(ma)]$–Cyt	12932.2	12934.2
$\{2[V^{IV}O(ma)]+[V^{IV}O(ma)_2]\}$–Cyt	13058.2	13059.2

4[$V^{IV}O$(ma)]–Cyt	13123.2	13126.1
{3[$V^{IV}O$(ma)]+[$V^{IV}O$(ma)$_2$]}–Cyt	13250.2	13251.2
5[$V^{IV}O$(ma)]–Cyt	13314.2	13318.1
{4[$V^{IV}O$(ma)]+[$V^{IV}O$(ma)$_2$]}–Cyt	13441.1	13443.1
[$V^{V}O_2$]–Cyt	12440.3	12441.2
[$V^{V}O_2$(ma)]–Cyt	12567.3	12566.3
{[$V^{V}O_2$(ma)]+$V^{V}O_2$}–Cyt	12649.4	12649.2
2[$V^{V}O_2$(ma)]}–Cyt	12775.3	12774.2
{2[$V^{V}O_2$(ma)]+$V^{V}O_2$}–Cyt	12856.2	12857.2
3[$V^{V}O_2$(ma)]}–Cyt	12983.5	12982.2

[a] The expected mass is obtained by summing the mass of the vanadium moiety to the experimental mass of the free protein (12358.3 Da).

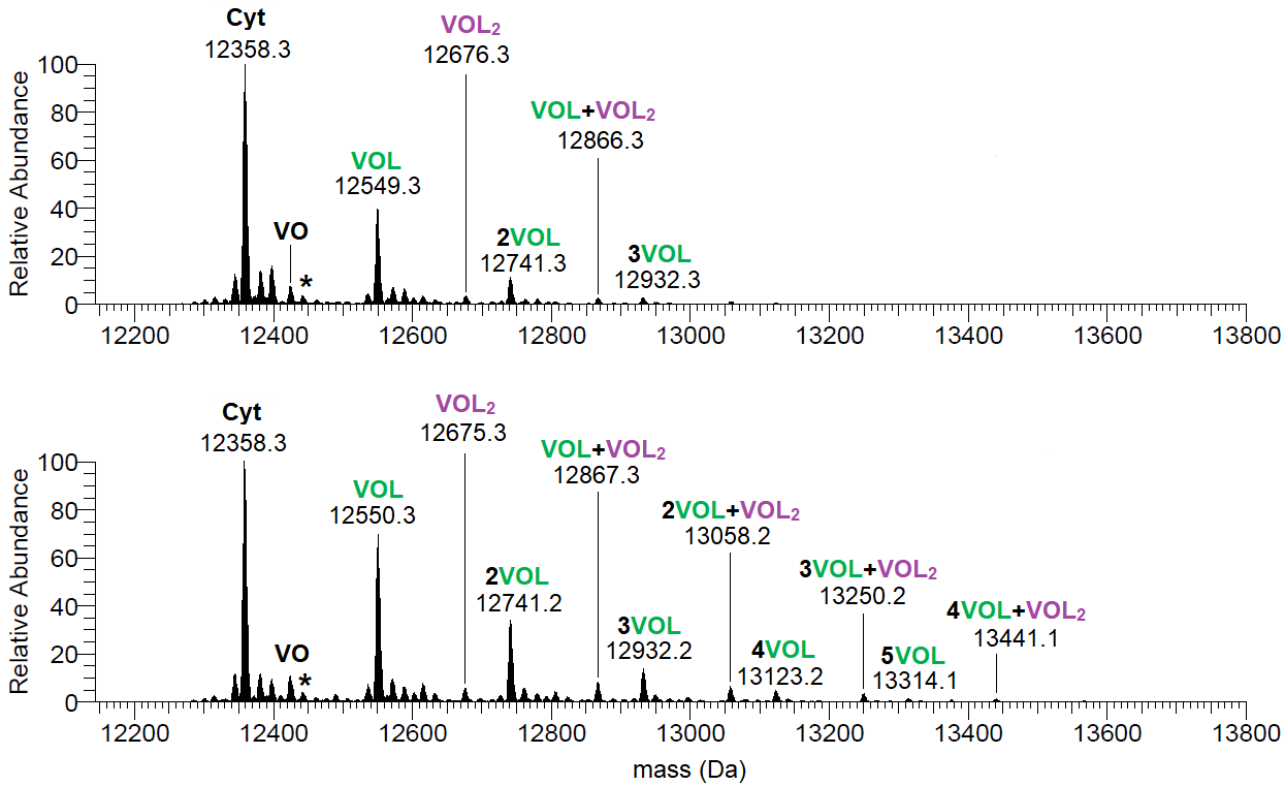

Figure 6. Deconvoluted ESI-MS spectra recorded on the system containing $V^{IV}O^{2+}$/ma 1/2 and cytochrome *c* (50 μM): V/Protein molar ratio 3/1 (top) and 5/1 (bottom). L indicates the maltolato ligand. With the asterisk the peak of the adduct [$V^{V}O_2$]−Cyt is denoted.

In the system with $V^{V}O_2$, ma and Cyt, studied with protein concentration of 5 or 50 μM and ratio

V/Cyt of 3/1 and 5/1, the ESI-MS spectra show the signals of the adducts formed by $V^{V}O_2^+$ (+82 Da compared to the mass of the protein) and $V^{V}O_2$(ma) (+209 Da). With increasing the protein concentration, up to 3 moieties $V^{V}O_2$(ma) can bind to the protein forming the adduct *n*[$V^{V}O_2$(ma)]–Cyt with *n* = 1-3 (Figure 7). Moreover, the peaks of the adducts {*n*[$V^{V}O_2$(ma)]+$V^{V}O_2$}–Cyt with *n* = 1-2, were detected.

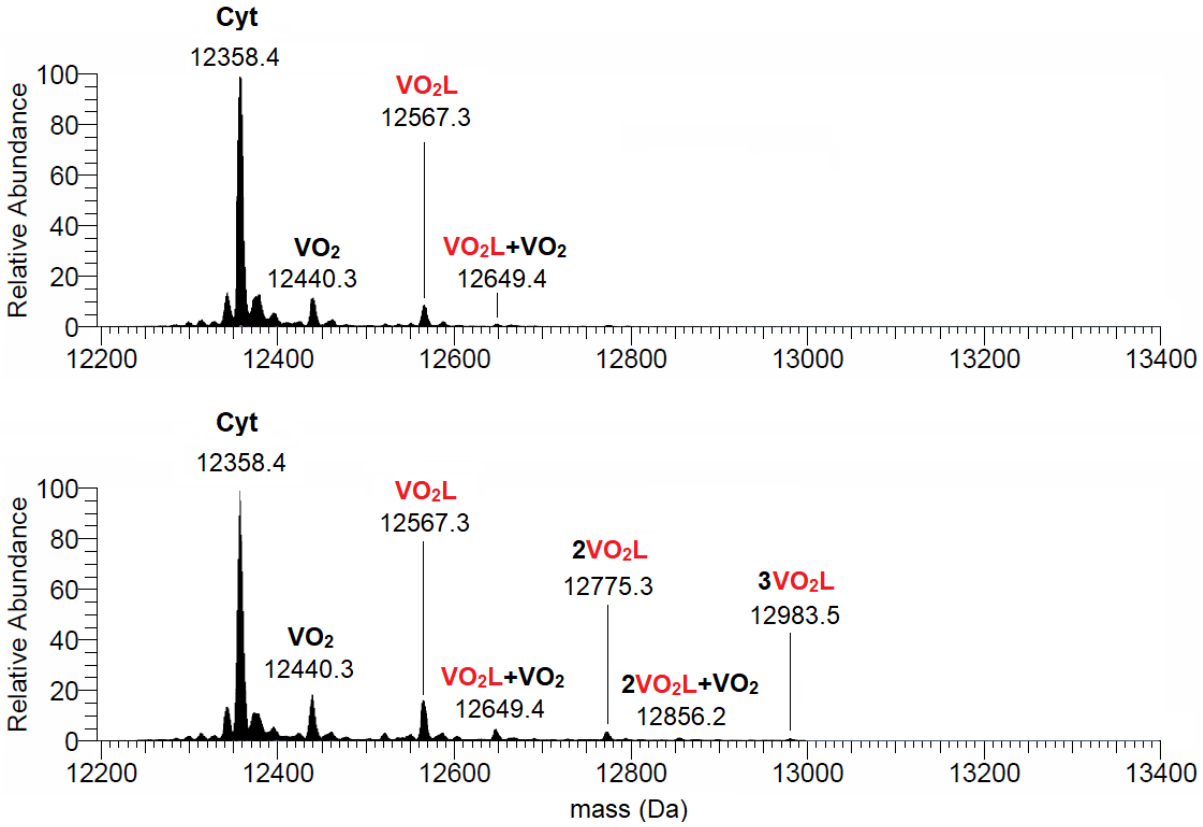

Figure 7. Deconvoluted ESI-MS spectra recorded on the system containing $V^{V}O_2^+$/ma 1/2 and Cytochrome *c* (50 µM): V/Protein molar ratio 3/1 (top) and 5/1 (bottom). L indicates the maltolato ligand.

3.5. Discussion of the ESI-MS data

In both the systems $V^{IV,V}$/L, with L = dhp or ma, several adducts with cytochrome *c* were observed with the moieties $V^{IV}OL_2$, $V^{IV}OL$, $V^{V}O_2L$ and $V^{V}O_2$. The formation of such adducts depends on several factors, mainly the V oxidation state, the ligand, the metal concentration and coordination geometry. The most important experimental observations can be summarized as follows.

1) In the case of systems with V^{IV}, the results are similar to those previously obtained with lysozyme [80]. Specifically, maltol forms adducts mainly with the moiety $V^{IV}O$(ma), while dhp with both $V^{IV}O$(dhp) and $V^{IV}O(dhp)_2$ fragments. These results are in agreement with the greater

strength of dhp ligand than ma (pK_a = 9.76 for Hdhp and 8.44 for Hma [69, 85]) and with the higher thermodynamic stability of bis-chelated $V^{IV}O$-dhp complexes [69, 85].

2) When vanadium(IV,V) complexes are compared, the general rule is that their stability decrease from V^{IV} to V^{V} [89], and the behavior of dhp and ma does not represent an exception. Therefore, in the case of V^{V} species, the formation of adducts with the 1:1 mono-chelated moieties and with the ion $V^{V}O_2^+$ is favored. For example, with V^{IV} the adducts are observed with 1:2 bis-chelated moiety of dhp (and, in small amount, of ma), while only the species $[V^{V}O_2(dhp)]$–Cyt and $[V^{V}O_2(ma)]$–Cyt are detected with V^{V}. Moreover, with vanadium(V), $[V^{V}O_2]$–Cyt, derived from the hydrolysis of the complexes, is revealed in both the systems; notably, the signals of this adduct are more intense when starting with $[V^{V}O_2(ma)_2]^-$ instead of $[V^{V}O_2(dhp)_2]^-$, which forms more stable complexes.

3) As expected, the decrease of the metal concentration favors the hydrolysis and the spectra recorded with V 15 or 25 μM show mainly the presence of $V^{IV}OL$ or $V^{V}O_2L$ (plus $V^{V}O_2$) instead of $V^{IV}OL_2$ or $V^{V}O_2L_2$ bound to cytochrome *c*.

4) The interaction of $[V^{V}O_2L_2]^-$ is not favored due to the saturation of the V coordination sphere that precludes the formation of covalent bonds. This means that, in the systems containing $[V^{V}O_2L_2]^-$, the non-covalent binding, observed for $V^{IV}O$ complexes of flavonoids [90], is not strong enough to stabilize the possible adducts. Notably, when Cyt is 50 μM, only the species $n[V^{V}O_2(ma)]$–Cyt were detected, even if – under these experimental conditions – the percent amount of $[V^{V}O_2(ma)_2]^-$ is larger than $[V^{V}O_2(ma)(OH)]^-$; for example, when the concentration of V^{V} is 150 μM, the respective percent amounts of the bis- and mono-chelated species are 27.7% and 5.8%, obtained on the thermodynamic stability constants reported in the literature [88].

5) Dhp forms adducts both with $V^{IV}O(dhp)$, with two adjacent equatorial sites for the protein binding, and $V^{IV}O(dhp)(H_2O)$ which has only one available site. In contrast, with ma, only adducts $[V^{IV}O(ma)]$–Cyt are detected.

6) Finally, species with composition $\{n[V^{IV}O(dhp)_2]+[V^{IV}O(dhp)]\}$–Cyt and $\{n[V^{IV}O(dhp)_2]+[V^{IV}O(dhp)(H_2O)]\}$–Cyt are revealed with dhp, and adducts $\{n[V^{IV}O(ma)]+[V^{IV}O(ma)_2]\}$–Cyt and $\{n[V^{V}O_2(ma)]+V^{V}O_2\}$–Cyt are formed by ma, suggesting that the protein can bind simultaneously two different moieties.

The analysis of cytochrome *c* allows to unveil interesting features on its binding capability. The residues that interact favorably with vanadium species are Asp and Glu with their carboxylate group and His with imidazole nitrogen [18, 44, 62]. Cyt has three Asp (Asp2, Asp50, Asp93), nine Glu (Glu4, Glu21, Glu61, Glu62, Glu66, Glu69, Glu90, Glu92, Glu104), and three His residues (His18, His26, His33, with His18 engaged in the Fe^{3+} binding) (Figure 8). Most of them are able to bind $V^{IV,V}$ only in a monodentate manner. A study of the surface residues of cytochrome *c* (structure

with code 1HRC [74] in Protein Data Bank (PDB)) with the software Swiss-Pdb Viewer [75] shows that, selecting 35% as the threshold value for considering an amino acid accessible for vanadium coordination, Asp2, Glu4, Glu21, His33, Asp50, Glu62, Glu66, Glu92, Asp93 and Glu104 are the most exposed residues (in blue or red in Figure 8). Notably, Glu21 (and Glu90) was predicted by docking calculations as a possible donor for the moiety *cis*-$V^{IV}O(nalidixato)_2$ [46], derived from the antibacterial compound *cis*-$[V^{IV}O(nalidixato)_2(H_2O)]$ [2]. Among the residues mentioned above, (Asp2, Glu4), (His33, Glu104) and (Glu92, Asp93) can bind simultaneously $V^{IV,V}$, realizing a bidentate coordination (in red in Figure 8).

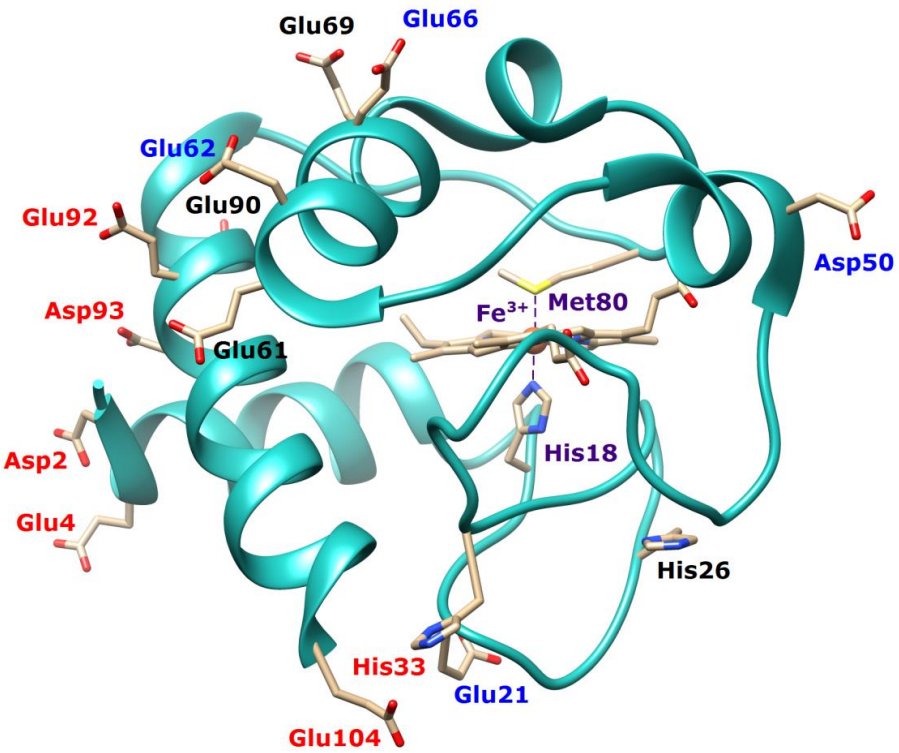

Figure 8. Structure of cytochrome *c* with all the Asp, Glu and His residues. The residues which can potentially bind $V^{IV,V}$ with a monodentate coordination are drawn in blue, while those which can be involved both in a monodentate and in a bidentate coordination are drawn in red. The site with Fe^{3+} ion and the apical His18 and Met80 residues is shown in purple.

The structure of the possible species formed by dhp and ma is represented in Scheme 2. Only dhp forms adducts with the stoichiometry $[V^{IV}OL_2]$–Cyt (Scheme 2c) and the interacting residue may be one among those with potential monodentate coordination (displayed in blue or red in Figure 8). Similarly, with the fragment $V^{IV}O(dhp)(H_2O)$, in which only one equatorial coordination site is available (Scheme 2e), the monodentate binding of the same residues seems to be plausible. The

other $V^{IV}O$ moieties, $V^{IV}O$(dhp) and $V^{IV}O$(ma) (Scheme 2d and 2g), have two free equatorial sites and both the mono- and bidentate coordination is possible. As pointed out above, the couples of residues with the right distance for a simultaneous $V^{IV,V}$ binding are (Asp2, Glu4), (Glu92, Glu93), and (His33, Glu104) (in red in Figure 8). With $V^{V}O_2$(dhp) and $V^{V}O_2$(ma) (Scheme 2f and 2h), the binding of only one amino acid residue in the equatorial position or two, one equatorial and one axial, is expected. Finally, $V^{V}O_2^{+}$ and $V^{IV}O^{2+}$ (Scheme 2a and 2b) have three and four free sites on the metal equatorial plane and, for them as well, two options are possible: the monodentate coordination of one accessible residue on the protein surface or the bidentate binding by two side-chains in the correct position to occupy two adjacent sites. For the free ions, however, the bidentate coordination seems more probable because it results in a significant increase of thermodynamic stability of the adduct and because their steric hindrance is much lower than $V^{IV}OL$ and $V^{V}O_2L$ fragments. The remaining positions should be occupied by H_2O and/or OH^{-} ligands.

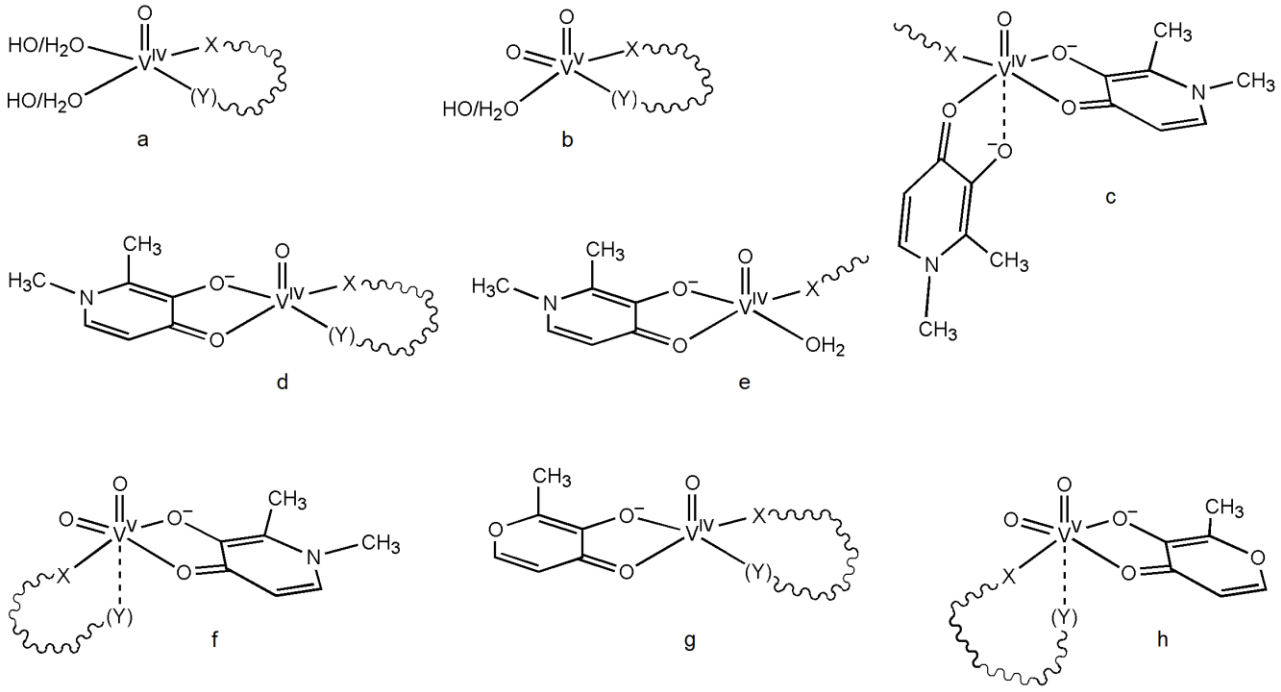

Scheme 2. Structure of the adducts formed by $V^{IV}O^{2+}$ and $V^{V}O_2^{+}$ ions and by $V^{IV,V}$ complexes of dhp and ma with cytochrome *c*. X indicates a donor belonging to one of the residues Asp2, Glu4, Glu21, His33, Asp50, Glu62, Glu66, Glu92, Asp93 and Glu104. When the binding of a second residue (Y) adds to the first one X, then X and Y are the couples (Asp2, Glu4), (Glu92, Glu93), and (His33, Glu104).

3.6. Electrochemical studies

As mentioned in the Introduction, in biological fluids a vanadium compound can undergo redox processes and the interconversion of the oxidation states +IV and +V is possible. Therefore, when a $[V^{IV}OL_2]$ drug is administered, the oxidation to $[V^{V}O_2L_2]^-$ must be considered. Subsequently, depending on pH and V concentration, other transformations like, for example, hydrolysis to give $V^{IV}OL^+/V^{V}O_2L$ or the corresponding hydroxido complexes $V^{IV}OL(OH)/V^{V}O_2L(OH)^-$ may occur.

The redox potential of the couple V^{IV}/V^{V} ($E_{1/2}$) for $[V^{IV}O(dhp)_2]$ was not univocally determined and a value of +0.67 V (vs. SHE) [81] or between 0.2 and 0.5 V (vs. Ag/AgCl electrode), as a function of pH, have been reported [91]. On the other hand, the $E_{1/2}$ potential in aqueous solution of $[V^{IV}O(ma)_2]$ to V^{V} is 0.45 V (vs. Ag/AgCl electrode) and 0.54 V (vs. SHE) at pH > 5.0 [70, 81]. A pH dependence was observed, which has been attributed to the existence of various complexes in solution [91].

In this study, the redox behavior of $[V^{IV}O(dhp)_2]$ and $[V^{IV}O(ma)_2]$ was reconsidered, taking into account that the dispersion of the $E_{1/2}$ values may be due to the presence of more than one species in solution [69, 85]. So, the cyclic voltammograms were recorded at pH where the concentration of 1:2 species reaches the maximum values. The CV's for the bis-chelated species are reported in Figure 9. In the systems containing $[V^{IV}O(dhp)_2]/[V^{IV}O(dhp)_2(H_2O)]$ and $[V^{IV}O(ma)_2(H_2O)]$ (see Scheme 1 for the structure of the species existing in aqueous solution), an anodic peak in the range 0.35-0.42 V is due to the oxidation of $V^{IV}O^{2+}$ to $V^{V}O_2^+$. After the scan direction is reverted, a cathodic peak is detected between 0.25 and 0.31 V, assigned to the reduction of the electrochemically generated $[V^{V}O_2(dhp)_2]^-$ and $[V^{V}O_2(ma)_2]^-$ at the electrode surface. The $E_{1/2}$ are very similar and are listed in Table 5; $E_{1/2}$ is 0.296 V vs. SCE for $[V^{IV}O(dhp)_2]/[V^{IV}O(dhp)_2(H_2O)]$ and 0.359 V for $[V^{IV}O(ma)_2(H_2O)]$. If these values are expressed vs. SHE, they do not differ significantly compared to the $E_{1/2}$ previously reported (Table 5). The results indicate that the oxidation is more favored for dhp than for ma species. The peak separation ΔE_p is 0.105 V (dhp) and 0.107 V (ma) and the value i_{pa}/i_{pc} is 1.35 (dhp) and 1.15 (ma), indicating an almost reversible process [92]. Overall, the electrochemical behavior can be interpreted considering the similarity of the structure of *cis*-$[V^{IV}OL_2(H_2O)]$ (L = dhp, ma; Scheme 1) and their oxidation product $[V^{V}O_2L_2]^-$: the $V^{IV}O(OH_2)$ group is oxidized to the $V^{V}O_2$ group through the reversible process:

$$V^{IV}O(OH_2)^{2+} \rightleftarrows V^{V}O_2^+ + 2H^+ + e^- \quad (1)$$

For comparison, the CV's of the hydroxido species $[V^{IV}O(dhp)_2(OH)]^-$ and $[V^{IV}O(ma)_2(OH)]^-$ were recorded at basic pH, 11.0 for the dhp system and 9.5 for maltol. The values of $E_{1/2}$ change slightly

for dhp complex (0.27 V vs. SCE) and a little more for ma species (0.54 V vs. SCE). However, the most significant experimental variation is the loss of reversibility of the redox process. This could be ascribed to the low amount of H^+ in solution at the explored pH, necessary to convert the oxido ligand O^{2-} of the $V^{V}O_2$ complex to H_2O of the $V^{IV}O$ derivative in eq. (1).

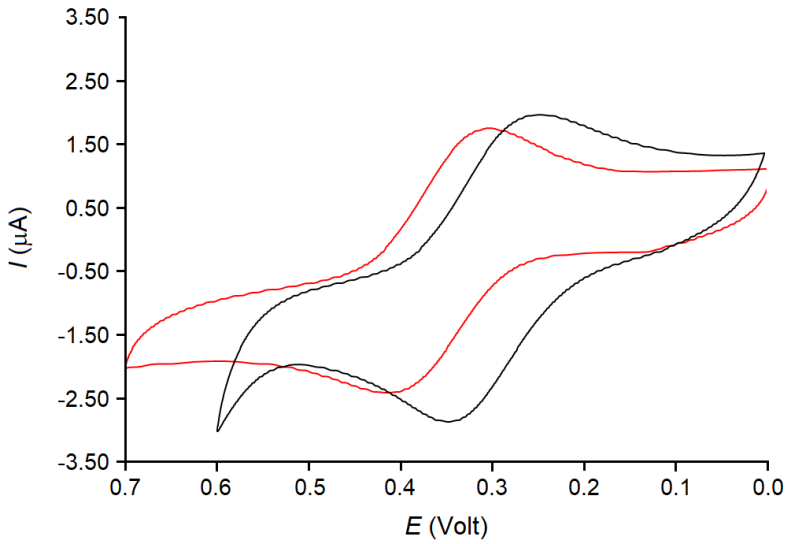

Figure 9. Cyclic voltammograms of $[V^{IV}O(ma)_2(H_2O)]$ (in red; $V^{IV}O$/ma 1/2, V^{IV} concentration 1 mM, pH 5.0) and $[V^{IV}O(dhp)_2)]/[V^{IV}O(dhp)_2(H_2O)]$ (in black; $V^{IV}O$/dhp 1/2, V^{IV} concentration 1 mM, pH 5.0). Glassy carbon was used as the working electrode and the potential *E* was measured vs. Hg/Hg_2Cl_2 electrode reference.

Table 5. Electrochemical data for the $V^{IV,V}$ complexes of dhp and ma.

	$E_{1/2}$[a]				
	This work	Ref. [81]	Ref. [91]	Ref. [70]	Behavior
$[V^{IV}O(dhp)_2]/[V^{IV}O(dhp)_2(H_2O)]$ [b]	0.53 V	0.67 V	0.6-0.9 V	–	Almost reversible
$[V^{IV}O(dhp)_2(OH)]^-$ [c]	0.51 V	–	–	–	Irreversible
$[V^{IV}O(ma)_2(H_2O)]$ [d]	0.60 V	0.54 V	–	< 0.64 V	Almost reversible
$[V^{IV}O(ma)_2(OH)]^-$ [e]	0.78 V	–	–	–	Irreversible

[a] All the values were referred to the standard hydrogen electrode (SHE). [b] $V^{IV}O$ concentration 1 mM, pH 5.0 [c] $V^{IV}O$ concentration 1 mM, pH 11.0. [d] $V^{IV}O$ concentration 1 mM, pH 5.0. [e] $V^{IV}O$ concentration 1 mM, pH 9.5.

3.7. Biological implications

The results obtained with ESI-MS and electrochemical studies allow us to get insights on the behavior of $[V^{IV}O(dhp)_2]$ and $[V^{IV}O(ma)_2]$ in biological fluids. As pointed out in the Introduction section, the oxidation state of V under physiological conditions has not been univocally determined, but an interconversion between the states +IV and +V seems to be possible in serum and cytosol and an equilibrium between the concentration of V^{IV} and V^{V} could be reached [11, 27, 38-43]. It has been demonstrated that on one hand $V^{IV}OL_2$ complexes can be oxidized to V^{V}; for example, BMOV is oxidized by molecular oxygen under ambient conditions in alcoholic solutions to form *cis*-$[V^{V}O(OR)(ma)_2]$ [93] and potentiometric and ^{51}V NMR measurements in the system V^{V}/ma at different pH revealed that the reduction to V^{IV} can take place below pH 4 [70]. On the other hand, the reduction of the corresponding V^{V} species may occur in the presence of reductants, such as reduced glutathione and ascorbic acid [43, 81], and in red blood cells [56, 94].

The values of $E_{1/2}$ could account for the decrease reduction of the intensity of the EPR signals detected in the time range 0-3 h at 37 °C in real serum samples containing the two complexes [95]. Moreover, they could explain why, under these conditions, the oxidation is faster for $[V^{IV}O(dhp)_2]$ (after 60 min the amount of V^{IV} is around 5%, while for longer times the spectral signal completely disappear) than for $[V^{IV}O(ma)_2]$ (35% of V^{IV} after 60 min and 20% after 180 min) [95]. For the sake of completeness, it must be mentioned that the major weak point of these experiments is that they were performed with blood exposed to air and, therefore, the concentration of molecular oxygen could exceed 40 mm Hg of the blood vessels [27]. Therefore, even if the debate is still open, it is plausible that a partial oxidation occurs and that an equilibrium between V^{IV} to V^{V} is reached *in vivo*.

The presence of a protein can alter these reactions and stabilize or destabilize one of the two oxidation states. In addition, it must be remembered that $V^{IV}O$ are generally more stable than the corresponding $V^{V}O_2$ complexes [43, 89]. We showed in this study that both $V^{IV,V}$–dhp and $V^{IV,V}$–ma complexes interact with Cyt, but – as expected – with vanadium(IV) the binding of $V^{IV}O(dhp)_2$/$V^{IV}O(dhp)$ and $V^{IV}O(ma)$ is observed, while with vanadium(V) only that of $V^{V}O_2(dhp)$ and $V^{V}O_2(ma)$ plus the free ion $V^{V}O_2^{+}$ is revealed. Obviously, the interaction of $V^{V}O_2^{+}$, $V^{V}O_2L$, $V^{IV}OL$ and $V^{IV}OL_2$ results in the formation of adducts with different thermodynamic stability. The strength of the interaction depends on several factors, among which the oxidation state of vanadium, +IV or +V, the possibility of the simultaneous coordination of a couple of side-chain donors (that, as observed above, is possible for cytochrome *c* with the couples (Asp2, Glu4), (Glu92, Glu93), and (His33, Glu104), but that can occur with other proteins [44, 45]), and stabilization of secondary interactions such as hydrogen bonds and/or van der Waals contacts [44, 96]. For these reasons, the

formed adducts would contribute to a different extent to the transport of the active V species in blood and to the uptake by the target cells. These findings reinforce the conclusion that several issues are necessary to explain the biological action of vanadium compounds: i) the transformation in fluids of organism [18, 39-41, 97-99], taking into account that this is not limited to the ligand exchange and hydrolysis but must include the redox reactions; ii) a mixture of species in the oxidation +IV and +V could be responsible of the pharmacological effects [43, 100].

4. Conclusions

The identification of the active species generated in the organism by the biotransformation of potential vanadium drugs is still a question mark. Some authors pointed out that the limited knowledge of these active species has strongly limited the tests and development of vanadium drugs [25], despite many *in vivo* experiments demonstrated their promising activity [9]. While it has been accepted that ligand exchange and hydrolysis are very important issues related to the action of biologically active compounds [40, 97, 99, 101], the interconversion of the V oxidation states +IV and +V in blood and cellular environment is a topic of intense debate. In fact, V^{IV} could be partly oxidized in blood by molecular oxygen and hydrogen peroxide, but the situation completely changes in cellular environment where V^{V} may be reduced to V^{IV} by GSH and ascorbic acid. Recent experiments pointed out that, among three potential reducing agents, ascorbate is more effective than GSH and, also, than NADH [43]. The tendency to the reduction/oxidation depends on the $E_{1/2}$ value, but several biomolecules may change such values stabilizing V^{IV} or V^{V}. So, there is an unanimous consensus that, under physiological conditions, an equilibrium between V^{IV} and V^{V} is reached [11, 27, 38-44].

The presence of a protein can alter these reactions and stabilize or destabilize one of the two most important oxidation states in the biological fluids. The strength of the binding to the proteins depends on the vanadium oxidation state (+IV or +V), on the stability of the metal complex, on the protein conformation and possibility of simultaneous coordination of a couple of side-chain donors [44, 45], and, also, by the type of bond (covalent or non-covalent) [44]. The oxidation state determines the stability of the V complexes, and $V^{IV}O$ are generally more stable than the corresponding $V^{V}O_2$ species [43, 89]; the data obtained in this study suggest that with V^{IV} is favored the interaction with the moieties $V^{IV}OL_2$ or $V^{IV}OL^{+}$, while with V^{V} that with the inorganic ion $V^{V}O_2^{+}$ or $V^{V}O_2L$ fragment. The formed adducts can be stabilized by secondary interactions such as hydrogen bonds or van der Waals contacts, in their turn related to the structure of the protein and of the ligand.

When a $[V^{IV}OL_2]$ or a $[V^{V}O_2L_2]^-$ complex is administered, a mixture of species like $V^{IV}OL^+$, $V^{IV}OL_2$, $V^{V}O_2^+$ and $V^{V}O_2L$ could exist, together with the hydrolyzed complexes such as $(V^{IV}O)_2(OH)_5^-$ and $V^{IV}O(OH)_3^-$ and $H_2V^{V}O_4^-/HV^{V}O_4^{2-}$, $H_2V^{V}_2O_7^{2-}/HV^{V}_2O_7^{3-}$ and $V^{V}_4O_{12}^{4-}$. Each of them could interact with the proteins of blood and cytosol. Therefore, it is plausible that both $V^{IV,V}$ species and $V^{IV,V}$–protein adducts may contribute (probably to a different extent) to the transport of potential V drugs in blood, to the uptake by the target cells and to the overall pharmacological action. These comments suggest that the biological action of vanadium drugs must be explained not only with the ligand exchange and hydrolysis at low metal concentration, as highlighted in the literature [18, 39-41, 97-99], but also with the redox processes which could bring to a mixture of V^{IV} and V^{V} active species.

Author Statement

Valeria Ugone: Investigation, Writing – original and revised manuscript. **Federico Pisanu**: Investigation, Writing – original and revised manuscript. **Eugenio Garribba**: Conceptualization, Supervision, Writing – original and revised manuscript, Funding acquisition.

Conflicts of interest

There are no conflicts of interest to declare.

Supplementary Material

Supplementary data to this article can be found online at http://dx.doi.org/10.1016/j.jinorgbio.2021.xx.xxx.

Acknowledgements

The authors thank Regione Autonoma della Sardegna (grant RASSR79857) and Fondazione di Sardegna (grant FdS2017Garribba) for the financial support. They are also grateful to Dr. Daniele Sanna (Istituto di Chimica Biomolecolare, Consiglio Nazionale delle Ricerche) for his valuable suggestions in the preparation of the manuscript.

5. References

[1] D. Gambino, Coord. Chem. Rev. 255 (2011) 2193-2203.

[2] B. Bueloni, D. Sanna, E. Garribba, G.R. Castro, I.E. León, G.A. Islan, Int. J. Biol. Macromol. 161 (2020) 1568-1580.

[3] K.H. Thompson, C. Orvig, J. Inorg. Biochem. 100 (2006) 1925-1935.

[4] K.H. Thompson, J. Lichter, C. LeBel, M.C. Scaife, J.H. McNeill, C. Orvig, J. Inorg. Biochem. 103 (2009) 554-558.

[5] D.C. Crans, L. Henry, G. Cardiff, B.I. Posner, Developing Vanadium as Antidiabetic and Anticancer Drugs: A Clinical and Historical Perspective in: P.L. Carver (Ed.) Essential Metals in Medicine: Therapeutic Use and Toxicity of Metal Ions in the Clinic, De Gruyter GmbH, Berlin, 2019, pp. 203-230.

[6] S. Treviño, A. Díaz, E. Sánchez-Lara, B.L. Sanchez-Gaytan, J.M. Perez-Aguilar, E. González-Vergara, Biol. Trace Elem. Res. 188 (2019) 68-98.

[7] S. Treviño, A. Diaz, J. Inorg. Biochem. 208 (2020) 111094.

[8] A.M. Evangelou, Crit. Rev. Oncol. Hematol. 42 (2002) 249-265.

[9] J. Costa Pessoa, S. Etcheverry, D. Gambino, Coord. Chem. Rev. 301-302 (2015) 24-48.

[10] E. Kioseoglou, S. Petanidis, C. Gabriel, A. Salifoglou, Coord. Chem. Rev. 301-302 (2015) 87-105.

[11] D. Crans, C, L. Yang, A. Haase, X. Yang, Health Benefits of Vanadium and Its Potential as an Anticancer Agent, in: A. Sigel, H. Sigel, E. Freisinger, R.K.O. Sigel (Eds.) Metallo-Drugs: Development and Action of Anticancer Agents, De Gruyter GmbH, Berlin, 2018, pp. 251-280.

[12] D. Rehder, Future Med. Chem. 4 (2012) 1823-1837.

[13] D. Rehder, Future Med. Chem. 8 (2016) 325-338.

[14] I.E. Leon, J.F. Cadavid-Vargas, V. Di, Ana Laura , S.B. Etcheverry, Curr. Med. Chem. 24 (2017) 112-148.

[15] D. Rehder, Inorg. Chim. Acta 504 (2020) 119445.

[16] C. Amante, A.L. De Sousa-Coelho, M. Aureliano, Metals 11 (2021) 828.

[17] M. Aureliano, N.I. Gumerova, G. Sciortino, E. Garribba, A. Rompel, D.C. Crans, Coord. Chem. Rev. 447 (2021) 214143.

[18] D. Sanna, E. Garribba, Curr. Med. Chem. 28 (2021) 1-46.

[19] T. Koleša-Dobravc, K. Maejima, Y. Yoshikawa, A. Meden, H. Yasui, F. Perdih, New J. Chem. 41 (2017) 735-746.

[20] T. Koleša-Dobravc, K. Maejima, Y. Yoshikawa, A. Meden, H. Yasui, F. Perdih, New J. Chem. 42 (2018) 3619-3632.

[21] J. Costa Pessoa, I. Tomaz, Curr. Med. Chem. 17 (2010) 3701-3738.

[22] K.D. Mjos, C. Orvig, Chem. Rev. 114 (2014) 4540-4563.

[23] M. Rangel, A. Tamura, C. Fukushima, H. Sakurai, J. Biol. Inorg. Chem. 6 (2001) 128-132.

[24] C. Rozzo, D. Sanna, E. Garribba, M. Serra, A. Cantara, G. Palmieri, M. Pisano, J. Inorg.

Biochem. 174 (2017) 14-24.
[25] T. Scior, J.A. Guevara-Garcia, Q.T. Do, P. Bernard, S. Laufer, Curr. Med. Chem. 23 (2016) 2874-2891.
[26] N.D. Chasteen, J.K. Grady, C.E. Holloway, Inorg. Chem. 25 (1986) 2754-2760.
[27] W.R. Harris, S.B. Friedman, D. Silberman, J. Inorg. Biochem. 20 (1984) 157-169.
[28] B. Frei, Y. Yamamoto, D. Niclas, B.N. Ames, Anal. Biochem. 175 (1988) 120-130.
[29] B. Halliwell, M.V. Clement, L.H. Long, FEBS Lett. 486 (2000) 10-13.
[30] S.D. Varma, P.S. Devamanoharan, Free Radical Res. Commun. 14 (1991) 125-131.
[31] H. Sakurai, S. Shimomura, K. Ishizu, Inorg. Chim. Acta 55 (1981) L67-L69.
[32] P.C. Wilkins, M.D. Johnson, A.A. Holder, D.C. Crans, Inorg. Chem. 45 (2006) 1471-1479.
[33] D.C. Crans, J.J. Smee, E. Gaidamauskas, L. Yang, Chem. Rev. 104 (2004) 849-902.
[34] D. Rehder, Bioinorganic Vanadium Chemistry, John Wiley & Sons, Ltd, Chichester, 2008.
[35] I.G. Macara, K. Kustin, L.C. Cantley Jr, Biochim. Biophys. Acta, Gen. Subj. 629 (1980) 95-106.
[36] T.V. Hansen, J. Aaseth, J. Alexander, Arch. Toxicol. 50 (1982) 195-202.
[37] H. Yasui, K. Takechi, H. Sakurai, J. Inorg. Biochem. 78 (2000) 185-196.
[38] D.C. Crans, Pure Appl. Chem. 77 (2005) 1497-1527.
[39] M. Le, O. Rathje, A. Levina, P.A. Lay, J. Biol. Inorg. Chem. 22 (2017) 663-672.
[40] A. Levina, D.C. Crans, P.A. Lay, Coord. Chem. Rev. 352 (2017) 473-498.
[41] A. Levina, P.A. Lay, Chem. Asian J. 12 (2017) 1692-1699.
[42] K.A. Doucette, K.N. Hassell, D.C. Crans, J. Inorg. Biochem. 165 (2016) 56-70.
[43] D. Sanna, J. Palomba, G. Lubinu, P. Buglyó, S. Nagy, F. Perdih, E. Garribba, J. Med. Chem. 62 (2019) 654-664.
[44] J. Costa Pessoa, M.F.A. Santos, I. Correia, D. Sanna, G. Sciortino, E. Garribba, Coord. Chem. Rev. 449 (2021) 214192.
[45] G. Sciortino, J.-D. Maréchal, E. Garribba, Inorg. Chem. Front. 8 (2021) 1951-1974.
[46] V. Ugone, D. Sanna, S. Ruggiu, G. Sciortino, E. Garribba, Inorg Chem Front 8 (2021) 1189-1196.
[47] G. Sciortino, E. Garribba, Chem. Commun. 56 (2020) 12218-12221.
[48] D. Sanna, G. Micera, E. Garribba, Inorg. Chem. 49 (2010) 174-187.
[49] D. Sanna, G. Micera, E. Garribba, Inorg. Chem. 52 (2013) 11975-11985.
[50] J. Costa Pessoa, G. Gonçalves, S. Roy, I. Correia, S. Mehtab, M.F.A. Santos, T. Santos-Silva, Inorg. Chim. Acta 420 (2014) 60-68.
[51] S. Mehtab, G. Gonçalves, S. Roy, A.I. Tomaz, T. Santos-Silva, M.F.A. Santos, M.J. Romão, T. Jakusch, T. Kiss, J. Costa Pessoa, J. Inorg. Biochem. 121 (2013) 187-195.
[52] I. Correia, I. Chorna, I. Cavaco, S. Roy, M.L. Kuznetsov, N. Ribeiro, G. Justino, F. Marques, T. Santos-Silva, M.F.A. Santos, H.M. Santos, J.L. Capelo, J. Doutch, J. Costa Pessoa, Chem. Asian J. 12 (2017) 2062-2084.
[53] G. Sciortino, D. Sanna, G. Lubinu, J.D. Marechal, E. Garribba, Chem. Eur. J. 26 (2020) 11316-

11326.
[54] E. Cobbina, S. Mehtab, I. Correia, G. Gonçalves, I. Tomaz, I. Cavaco, T. Jakusch, E. Enyedi, T. Kiss, J. Costa Pessoa, J. Mex. Chem. Soc. 57 (2013) 180-191.
[55] I. Correia, T. Jakusch, E. Cobbinna, S. Mehtab, I. Tomaz, N.V. Nagy, A. Rockenbauer, J. Costa Pessoa, T. Kiss, Dalton Trans. 41 (2012) 6477-6487.
[56] D. Sanna, M. Serra, G. Micera, E. Garribba, Inorg. Chem. 53 (2014) 1449-1464.
[57] D. Sanna, G. Micera, E. Garribba, Inorg. Chem. 50 (2011) 3717-3728.
[58] G. Sciortino, D. Sanna, V. Ugone, G. Micera, A. Lledós, J.-D. Maréchal, E. Garribba, Inorg. Chem. 56 (2017) 12938-12951.
[59] G. Sciortino, D. Sanna, V. Ugone, J.-D. Maréchal, M. Alemany-Chavarria, E. Garribba, New J. Chem. 43 (2019) 17647-17660.
[60] G. Sciortino, V. Ugone, D. Sanna, G. Lubinu, S. Ruggiu, J.-D. Maréchal, E. Garribba, Front. Chem. 8 (2020) 345.
[61] M.F.A. Santos, I. Correia, A.R. Oliveira, E. Garribba, J. Costa Pessoa, T. Santos-Silva, Eur. J. Inorg. Chem. 2014 (2014) 3293-3297.
[62] G. Sciortino, D. Sanna, V. Ugone, J.D. Marechal, E. Garribba, Inorg. Chem. Front. 6 (2019) 1561-1578.
[63] V. Ugone, D. Sanna, G. Sciortino, J.D. Marechal, E. Garribba, Inorg. Chem. 58 (2019) 8064-8078.
[64] G. Ferraro, N. Demitri, L. Vitale, G. Sciortino, D. Sanna, V. Ugone, E. Garribba, A. Merlino, Inorg. Chem. 60 (2021) 19098-19109.
[65] M. Wenzel, A. Casini, Coord. Chem. Rev. 352 (2017) 432-460.
[66] M. Šamalikova, I. Matečko, N. Müller, R. Grandori, Anal. Bioanal. Chem. 378 (2004) 1112-1123.
[67] G.C. Brown, V. Borutaite, Biochim. Biophys. Acta, Bioenerg. 1777 (2008) 877-881.
[68] L.J. Delinois, O. De León-Vélez, A. Vázquez-Medina, A. Vélez-Cabrera, A. Marrero-Sánchez, C. Nieves-Escobar, D. Alfonso-Cano, D. Caraballo-Rodríguez, J. Rodriguez-Ortiz, J. Acosta-Mercado, J.A. Benjamín-Rivera, K. González-González, K. Fernández-Adorno, L. Santiago-Pagán, R. Delgado-Vergara, X. Torres-Ávila, A. Maser-Figueroa, G. Grajales-Avilés, G.I.M. Méndez, J. Santiago-Pagán, M. Nieves-Santiago, V. Álvarez-Carrillo, K. Griebenow, A.D. Tinoco, Inorganics 9 (2021) 83.
[69] P. Buglyo, T. Kiss, E. Kiss, D. Sanna, E. Garribba, G. Micera, J. Chem. Soc., Dalton Trans. (2002) 2275-2282.
[70] C. Orvig, P. Caravan, L. Gelmini, N. Glover, F.G. Herring, H. Li, J.H. McNeill, S.J. Rettig, I.A. Setyawati, J. Am. Chem. Soc. 117 (1995) 12759-12770.
[71] E. Lodyga-Chruscinska, D. Sanna, E. Garribba, G. Micera, Dalton Trans. (2008) 4903-4916.
[72] H.M. Berman, J. Westbrook, Z. Feng, G. Gilliland, T.N. Bhat, H. Weissig, I.N. Shindyalov, P.E. Bourne, Nucleic Acids Res. 28 (2000) 235-242.
[73] S.K. Burley, H.M. Berman, C. Christie, J.M. Duarte, Z. Feng, J. Westbrook, J. Young, C.

Zardecki, Protein Sci. 27 (2018) 316-330.
[74] G.W. Bushnell, G.V. Louie, G.D. Brayer, J. Mol. Biol. 214 (1990) 585-595.
[75] N. Guex, M.C. Peitsch, Electrophoresis 18 (1997) 2714-2723.
[76] R.C. Hider, A.V. Hoffbrand, N. Engl. J. Med. 379 (2018) 2140-2150.
[77] J. Burgess, B. De Castro, C. Oliveira, M. Rangel, W. Schlindweind, Polyhedron 16 (1997) 789-794.
[78] M. Rangel, A. Leite, M.J. Amorim, E. Garribba, G. Micera, E. Lodyga-Chruscinska, Inorg. Chem. 45 (2006) 8086-8097.
[79] D. Sanna, G. Lubinu, V. Ugone, E. Garribba, Dalton Trans. 50 (2021) 16326-16335.
[80] V. Ugone, D. Sanna, G. Sciortino, D.C. Crans, E. Garribba, Inorg. Chem. 59 (2020) 9739-9755.
[81] T. Jakusch, É.A. Enyedy, K. Kozma, Z. Paár, A. Bényei, T. Kiss, Inorg. Chim. Acta 420 (2014) 92-102.
[82] A. Casini, C. Gabbiani, G. Mastrobuoni, L. Messori, G. Moneti, G. Pieraccini, ChemMedChem 1 (2006) 413-417.
[83] J.B. Fenn, J. Am. Soc. Mass Spectrom. 4 (1993) 524-535.
[84] A. Dobo, I.A. Kaltashov, Anal. Chem. 73 (2001) 4763-4773.
[85] P. Buglyo, E. Kiss, I. Fabian, T. Kiss, D. Sanna, E. Garribba, G. Micera, Inorg. Chim. Acta 306 (2000) 174-183.
[86] D. Sanna, P. Buglyo, L. Biro, G. Micera, E. Garribba, Eur. J. Inorg. Chem. (2012) 1079-1092.
[87] K. Elvingson, A. González Baró, L. Pettersson, Inorg. Chem. 35 (1996) 3388-3393.
[88] T. Jakusch, A. Dean, T. Oncsik, A.C. Bényei, V. Di Marco, T. Kiss, Dalton Trans. 39 (2010) 212-220.
[89] L.F. Vilas Boas, J. Costa Pessoa, Vanadium, in: G. Wilkinson, R.D. Gillard, J.A. McCleverty (Eds.) Comprehensive Coordination Chemistry, Pergamon Press, Oxford, 1987, pp. 453-583.
[90] G. Sciortino, D. Sanna, V. Ugone, A. Lledós, J.-D. Maréchal, E. Garribba, Inorg. Chem. 57 (2018) 4456-4469.
[91] M.M.C.A. Castro, C.F.G.C. Geraldes, P. Gameiro, E. Pereira, B. Castro, M. Rangel, J. Inorg. Biochem. 80 (2000) 177-179.
[92] P.T. Kissinger, W.R. Heineman, J. Chem. Educ. 60 (1983) 702.
[93] Y. Sun, B.R. James, S.J. Rettig, C. Orvig, Inorg. Chem. 35 (1996) 1667-1673.
[94] D. Sanna, M. Serra, G. Micera, E. Garribba, Inorg. Chim. Acta 420 (2014) 75-84.
[95] D. Sanna, V. Ugone, M. Serra, E. Garribba, J. Inorg. Biochem. 173 (2017) 52-65.
[96] M. Aureliano, N.I. Gumerova, G. Sciortino, E. Garribba, C.C. McLauchlan, A. Rompel, D.C. Crans, Coord. Chem. Rev. 454 (2022) 214344.
[97] J. Costa Pessoa, I. Correia, Inorganics 9 (2021) 17.
[98] P. Nunes, I. Correia, I. Cavaco, F. Marques, T. Pinheiro, F. Avecilla, J.C. Pessoa, J. Inorg. Biochem. 217 (2021) 111350.
[99] D. Sanna, V. Ugone, G. Micera, P. Buglyo, L. Biro, E. Garribba, Dalton Trans. 46 (2017)

8950-8967.
[100] A. Banerjee, S.P. Dash, M. Mohanty, G. Sahu, G. Sciortino, E. Garribba, M.F.N.N. Carvalho, F. Marques, J. Costa Pessoa, W. Kaminsky, K. Brzezinski, R. Dinda, Inorg. Chem. 59 (2020) 14042-14057.
[101] T. Jakusch, T. Kiss, Coord. Chem. Rev. 351 (2017) 118-126.